1   **Isolation and Gene Flow in a Speciation Continuum in Newts**

2

3   Maciej Pabijan [a,b,]*, Piotr Zieliński[a], Katarzyna Dudek[a], Michał Stuglik[a,c], Wiesław Babik[a]*

4   [a] *Institute of Environmental Sciences, Jagiellonian University, ul. Gronostajowa 7, 30-387,*

5   *Kraków, Poland* katarzyna2.dudek@uj.edu.pl, piotr.zielinski@uj.edu.pl

6   michal.stuglik@uj.edu.pl

7   [b] Permanent address: *Department of Comparative Anatomy, Institute of Zoology and Biomedical*

8   *Research, Jagiellonian University, ul. Gronostajowa 9, 30-387, Kraków, Poland*

9   [c] *Scotland's Rural College, Integrative Animal Sciences, Easter Bush Campus, Midlothian*

10   *EH25 9RG, Scotland, UK*

11   * Corresponding authors:

12   Maciej Pabijan, Department of Comparative Anatomy, Institute of Zoology and Biomedical

13   Research, Jagiellonian University, ul. Gronostajowa 9, 30-387, maciej.pabijan@uj.edu.pl

14   Wiesław Babik, Institute of Environmental Sciences, Jagiellonian University, ul. Gronostajowa

15   7, 30-387, Kraków, Poland**;** wieslaw.babik@uj.edu.pl

16   **Abstract**

17   Because reproductive isolation often evolves gradually, differentiating lineages may retain the

18   potential for genetic exchange for prolonged periods, providing an opportunity to quantify

19   and understand the fundamental role of gene flow during speciation. Here we delimit taxa,

20   reconstruct the phylogeny and infer gene flow in newts of the *Lissotriton vulgaris* species

21   complex based on 74 nuclear markers sampled from 127 localities. We demonstrate that

22   distinct lineages along the speciation continuum in newts exchange nontrivial amounts of

23   genes, affecting their evolutionary trajectories. By integrating a wide array of methods, we

24   delimit nine taxa and show that two principle factors have driven their genetic differentiation:

25   time since the last common ancestor determining levels of shared ancestral polymorphism,

26   and shifts in geographic distributions determining the extent of secondary contact. Post-

27   divergence gene flow, indicative of evolutionary non-independence, has been most extensive

28   between sister and non-sister taxa in Central Europe, while four southern European lineages

29   have acquired the population genetic hallmarks of independent species (*L. graecus*, *L.*

30   *kosswigi*, *L. lantzi*, *L. schmidtleri*). We obtained strong statistical support for widespread

31   mtDNA introgression, previously suggested by discordance between mtDNA phylogeny and

32   morphology. Our study suggests that long-term evolution in structured populations that may

33   periodically exchange genes may be common: although some of these populations may

34   become extinct or fuse, others will acquire complete reproductive isolation and will carry

35   signatures of this complex history in their genomes.

36   Key Words: delimitation, reticulate evolution, taxonomy, amphibian

37 1. **Introduction**

38 Speciation, regardless of the mechanisms or geographic settings in which it occurs, is

39 typically a gradual process (Coyne and Orr, 2004). The consequences of this are manifold.

40 First, we see various stages of speciation in nature which makes delimitation of separately

41 evolving units challenging (Huang and Knowles, 2016; Wiens, 2007). Second, completion of

42 speciation is by no means certain, other outcomes such as fusions or extinction are also likely

43 (e.g. Rhymer and Simberloff, 1996; Rudman and Schluter, 2016). Gene flow may

44 homogenize diverging gene pools (Petit and Excoffier, 2009; Slatkin, 1985), thereby limiting

45 or even reversing differentiation. Third, it is unclear how much gene flow occurs between

46 differentiating lineages, whether contact between such lineages causes massive introgression,

47 and to what extent introgression is heterogeneous throughout the genome (Cruikshank and

48 Hahn, 2014; Wolf and Ellegren, 2016).

49 Although theory provides some guidelines, the preceding questions are mostly

50 empirical and need to be addressed by studying natural systems. Recent spectacular adaptive

51 radiations may be less informative and more exceptional in this respect than commonly

52 assumed, because extinction may not have yet had sufficient time to prune the more

53 ephemeral products of divergent selection (Cutter and Gray, 2016). Therefore, careful

54 analyses of taxa composed of metapopulation lineages at various stages of divergence (de

55 Queiroz, 2007), which can be referred to as a speciation continuum, are needed. Because the

56 necessary analyses lie at the interface of population genetics and phylogenetics, they require

57 integration of tools from both fields. This is especially important for studies that explicitly

58 incorporate gene flow into the equation, because population genetic approaches for inferring

59 post-divergence gene flow are better developed than methods co-estimating phylogeny and

60 gene flow (Sousa and Hey, 2013). Likewise, accounting for post-divergence gene flow is a

61 major challenge for current species delimitation methods (Petit and Excoffier, 2009).

4

62   European newts from the *Lissotriton vulgaris* group provide an empirical example of a

63   speciation continuum influenced by genetic exchange between taxa. The Carpathian newt, *L.*

64   *montandoni* (Boulenger, 1880) and the smooth newt, *Lissotriton vulgaris* (Linnaeus, 1758),

65   have parapatric distributions in central Europe (Fig. 1a; Macgregor et al., 1990; Rafiński and

66   Arntzen, 1987). The former is endemic to the Carpathian and easternmost Sudetes mountains,

67   whereas the latter has a very large range in Central and Northern Europe, with a disjunct

68   population surrounding the Greater Caucasus mountains (Fig. 1a). At the intraspecific level,

69   *L. montandoni* is morphologically uniform across its range, reflected by only shallow genetic

70   substructuring (Zieliński et al., 2014). In sharp contrast, *L. vulgaris* is morphologically

71   differentiated into at least seven subspecies (Fig. 1a; Raxworthy, 1990). The smooth newt is

72   found in a variety of habitats across the collective ranges of the subspecies (Bour et al., 2002;

73   Bousbouras and Ioannidis, 1997; Schmidtler and Franzen, 2004; Skorinov et al., 2008) from

74   deciduous woodlands, farmlands and pastures in European lowlands and mountainous

75   regions, forest-steppe and taiga in western Siberia and Kazakhstan and pockets of humid

76   habitat in otherwise dry woodland or scrub in southern Europe and Anatolia. Despite over a

77   century of study, the status of the *L. vulgaris* subspecies is still controversial (Dubois and

78   Raffaëlli, 2009; Schmidtler and Franzen, 2004; Speybroeck et al., 2010; Wielstra et al., 2015).

79   The disagreement has been exacerbated by a general lack of concordance between

80   morphologically assessed subspecific boundaries and spatial patterns of mtDNA variation

81   (Fig. 1a, Fig. S1; Babik et al., 2005; Nadachowska and Babik, 2009; Pabijan et al., 2015). The

82   traits used to distinguish the smooth newt subspecies pertain almost exclusively to male

83   secondary sexual characters, which include the presence/absence and extent of dorsal crests

84   and tail fins, toe flaps, tail filament, dorso-lateral ridges and pigmentation patterns

85   (Raxworthy, 1990) that develop in aquatic habitats during the breeding season. Despite

86   divergent courtship behavior (Pecio and Rafiński, 1985) that leads to strong but incomplete

5

87 prezygotic sexual isolation between *L. montandoni* and *L. vulgaris* (Michalak and Rafiński,

88 1999; Michalak et al., 1997), these two species hybridize in and around the Carpathian

89 mountains forming a bimodal hybrid zone (Babik and Rafiński, 2004; Babik et al., 2003;

90 Kotlík and Zavadil, 1999). Hybridization has led to the replacement of the original mtDNA of

91 *L. montandoni* by introgressed mtDNA of several *L. vulgaris* lineages (Babik et al., 2005;

92 Zieliński et al., 2013). Moreover, genetic exchange among the different subspecies of *L.*

93 *vulgaris* is suggested because five of the subspecific taxa do not form monophyletic mtDNA

94 lineages (Fig. S1; Babik et al., 2005; Nadachowska and Babik, 2009; Pabijan et al., 2015).

95 Areas of subspecies intergradation with morphological intermediates have been reported in

96 central and southeastern Europe (e.g. Krizmanic et al., 1997; Schmidtler and Franzen, 2004;

97 Schmidtler and Schmidtler, 1983; Wielstra et al., 2015). These findings suggest that

98 introgressive hybridization both between *L. vulgaris* and *L. montandoni*, and among the

99 various subspecies of *L. vulgaris*, has the potential to blur boundaries among the different

100 taxa.

101 Here, we provide a multi-faceted perspective on divergence and gene flow in the *L.*

102 *vulgaris* complex. First, we postulate that morphologically diagnosable taxa within the

103 complex constitute separately evolving metapopulation lineages (de Quieroz, 2007) and test

104 this assertion using a clustering approach based on allele frequencies, a Bayesian multispecies

105 coalescent delimitation method, and the genealogical sorting index. Second, we hypothesize

106 that gene flow has blurred phylogenetic relationships and misled phylogeny reconstruction

107 methods that do not take reticulation explicitly into account (Leaché et al., 2014; Solís-Lemus

108 et al., 2016). Third, we predict that the extent of historical gene flow was most extensive

109 among lineages inhabiting Central Europe, and use an Approximate Bayesian Computation

110 framework to model gene flow between pairs of taxa. Finally, we apply the inferred nuclear

111 phylogeny to statistically test the previously proposed hypothesis of extensive mtDNA

112   introgression among morphologically diagnosable taxa. We demonstrate that isolation in

113   space and time as well as post-divergence gene flow shape the genetic background of a set of

114   metapopulations that have diverged in ecology and morphology including male epigamic

115   traits.

116   **2. Material and Methods**

117   2.1 Newt sampling

118   Tissues (tail-tips) were sampled from 127 newt populations (i.e. breeding sites, Table S1 and

119   Fig. 1b). Our sampling focused on capturing the genetic variation present in all

120   morphologically defined taxa within the *L. vulgaris* group and all potential Pleistocene

121   refugia (Babik et al., 2005; Nadachowska and Babik, 2009; Pabijan et al., 2015) and was

122   therefore mostly limited to southeastern and central Europe. Because the results of the current

123   study support the elevation of four taxa to the species level (see Discussion), we use this

124   updated nomenclature throughout the text. One individual was sampled per locality.

125   Altogether we analysed sequence data for 128 individuals (plus outgroup) which included 42

126   reported in Zieliński et al. (2016) and 87 sequenced for this study (Table S1).

127   2.2 Laboratory procedures and datasets

128   DNA from ethanol preserved tissues was extracted using either a standard phenol/chloroform

129   technique or the Wizard Genomic DNA extraction kit (Promega). Amplification and

130   sequencing of a panel of 74 nuclear, mostly 3'UTR markers, followed Zieliński et al. (2014).

131   This procedure resulted in physically phased sequences of both haplotypes for most markers

132   in most individuals. We used four different datasets for analyses (Table S2) i) dataset 1 with

133   sequences of all 74 loci and all 128 individuals, ii) dataset 2 with sequences of all 74 loci but

134   with 118 individuals (excluded 9 admixed individuals and one of two newts from locality

135   Kapakli), iii) dataset 3 with sequences of all 128 individuals but 70 loci (excluded 4 loci with

136   > 10% missing sequences), iv) dataset 4 consisting of SNPs extracted from 71 loci (excluded

137   loci with >10% missing data at nucleotide positions) and 120 individuals (including

138   outgroup).

139   2.3 Species delimitation

140   Species delimitation was based on identifying distinct genetic groups from haplotype

141   frequency data and validating the genetic clusters using multispecies coalescent-based and

142   genealogical sorting methods.

143   Sequence alignments (dataset 1) were converted into input for STRUCTURE v.2.3.4

144   (Pritchard et al., 2000) by coding each haplotype as a unique integer in a custom Python

145   script. If nucleotide sequences contained over 10 Ns or gaps, they were coded as missing data,

146   if they had less than 10 Ns or gaps, then columns with missing data were removed from the

147   alignment. This procedure ensured that haplotype identity was based on nucleotide

148   differences between sequences (and not on e.g. indels or low-quality data) and provided a

149   conservative estimate of the number of haplotypes per locus. STRUCTURE was run under the

150   admixture model ($\alpha = 1.0$) with independent allele frequencies among populations ($\lambda = 1.0$)

151   for K from 1 to 12, iterated 10 times each. The Markov chain in each analysis was set to 1

152   million burnin steps; a further 2 million steps were used for parameter value estimation.

153   STRUCTURE HARVESTER (Earl and vonHoldt, 2012) and CLUMPAK (Kopelman et al.,

154   2015) were used process the STRUCTURE output and to evaluate the most probable number

155   of clusters (K) by examining logPr($Data$).

156   We validated the genetic clusters identified by STRUCTURE by applying joint

157   Bayesian species delimitation and species tree estimation using the program BPP v3.1 (Yang,

158   2015). This approach is based on the multispecies coalescent and compares different models

159   of species delimitation and species phylogeny in a Bayesian framework, accounting for

160 incomplete lineage sorting and gene tree-species tree conflict (Rannala and Yang, 2013; Yang

161 and Rannala, 2010, 2014). Input alignments were constructed from dataset 2 by taking 10

162 sequences per marker for each of the 9 STRUCTURE-delimited operational taxonomic units

163 (hereafter OTUs). This sampling strategy was based on the minimum number of sequences

164 available per taxon (imposed by 5 specimens of *L. v. meridionalis*), with random subsampling

165 of 10 sequences (without replacement) in all other taxa. Admixed individuals (as defined by

166 STRUCTURE) were excluded from this analysis. We explored a wide variety of priors on the

167 population size parameters (θs) and divergence time at the root of the species tree (τ_0) (see

168 Extended Methods in the Supplementary Material).

169   Next, we estimated gene trees in MrBayes 3.2 (Ronquist et al., 2012) and used them as

170 input in Bayesian concordance analysis and an assessment of genealogical sorting (see

171 below). We applied dataset 3; outgroups consisted of a single, randomly chosen haplotype per

172 locus of a *Lissotriton helveticus* individual, or if unavailable due to lack of amplification, a

173 single haplotype from either *L. italicus* (for 3 markers) or *L. boscai* (for 9 markers) from

174 Zieliński et al. (2014). Nucleotide substitution models for each marker were determined in

175 jModeltest 2.1.4 (Darriba et al., 2012) under the Bayesian information criterion. Due to the

176 low phylogenetic information content of many of the markers, we did not partition the

177 alignments into codon positions for those containing coding regions. We implemented two

178 runs each with four chains for 3 million generations with trees and parameters sampled every

179 3000 generations. Convergence was assessed by comparing the –lnL values between runs and

180 by examining parameter values for a subset of markers in Tracer (Rambaut and Drummond,

181 2007). We discarded half of recorded gene trees as burnin, combined runs and constructed an

182 extended majority tree in MrBayes (allcompat command).

183   We quantified the genealogical distinctiveness of the OTUs by measuring exclusive

184 ancestry across gene trees with the genealogical sorting index (*gsi*) of Cummings et al.

9

185   (2008). This statistic measures the genealogical exclusivity of a grouping on a scale from 0

186   (random distribution of sequences among groups) to 1 (complete monophyly), and an

187   ensemble statistic (*egsi*) is used to integrate across gene trees. Because the *gsi* is sensitive to

188   disparity in group size, we randomly pruned leaves to a sample size of 10 (the minimum

189   number of sequences available per group). Admixed individuals were also pruned from gene

190   trees. We used the R implementation of the *gsi* (genealogicalSorting v.0.92). The null

191   hypothesis that the degree of exclusive ancestry of each group was observed by chance was

192   evaluated by 10^6 permutations.

193   2.4 Phylogeny estimation

194   Our first phylogenetic approach involved using individuals as taxonomic units and

195   concatenating the sequences of all loci. This procedure necessitates the selection of a single

196   haplotype per individual per marker and becomes non-trivial if that individual is heterozygous

197   at multiple loci, because the choice of which haplotype to concatenate into the matrix may

198   influence both the topology and branch support of resultant trees (Weisrock et al., 2012). For

199   each individual in dataset 2, we randomly merged haplotypes from each gene into two

200   concatenated sequences (i.e., each individual was represented by two entries of 36, 918 bp

201   consisting of 74 concatenated markers). We then pooled haplotypes for each candidate species

202   and randomly selected half of the haplotypes from each group for analysis. We followed

203   Weisrock et al. (2012) in conducting ten replicate analyses to assess consistency. We ran

204   mixed-model phylogenetic analyses in MrBayes 3.2 on the CIPRES Science Gateway

205   platform (Miller et al., 2010). We divided the alignments into 74 partitions corresponding to

206   markers and assigned the optimal nucleotide substitution models to these partitions as

207   previously determined by jModeltest. Each analysis consisted of two runs with 8 chains for 20

208   million generations with trees and parameters sampled every 5000 generations; burnin was set

209   at 50%. Convergence between runs was assessed by examining effective samples sizes and

210   parameter values between runs in Tracer, and by comparing topologies in AWTY (Nylander

211   et al., 2008).

212   The second phylogenetic method involved using BUCKy (Ané et al., 2007; Larget et

213   al., 2010) to estimate levels of concordance in reconstructed topologies among the posterior

214   distributions of gene trees generated in MrBayes. Because the number of unique tips per gene

215   tree was prohibitive (see Extended Methods), we pruned the gene trees in the MrBayes

216   posterior distributions by randomly selecting a single tip from each OTU using an R script

217   from Weisrock et al. (2012), modified to accommodate our dataset and subsampling

218   requirements. Admixed individuals were also pruned from gene trees. We tested a range of

219   priors and parameter values for BUCKy (see Extended Methods). We pruned the original

220   gene trees to 10 OTUs (9 candidate species plus outgroup) and repeated the subsampling and

221   pruning routine 50 times, using BUCKy to calculate the primary concordance trees for each

222   replicate. We measured clade support by calculating the mean ($\pm$ SD) sample-wide

223   concordance factors for clades across all 50 replicates. We also measured clade support by

224   computing the frequency with which each clade was recovered over all replicates.

225   We constructed a maximum likelihood tree using TreeMix 1.12 (Pickrell and

226   Pritchard, 2012) which uses a covariance matrix based on allele frequencies of SNPs to infer

227   the evolutionary relationships among pre-specified populations. The algorithm then identifies

228   populations more closely related than predicted by the phylogeny and adds a "migration

229   edge" between them, representing the direction and magnitude of gene flow (Pickrell and

230   Pritchard, 2012). We used the nine OTUs and an outgroup as populations. Note that allele

231   frequencies for our outgroup "population" were based on two gene copies because only one

232   outgroup individual was sequenced per marker (see single gene analyses above). We extracted

233   and sorted biallelic SNPs at each of the 74 markers according to minor allele frequency

234   (MAF). Five SNPs with the highest MAF, i.e. most informative at the level of the entire

235   dataset, were retrieved per marker, under the condition that they contained <10% missing data

236   at a nucleotide position; these positions were then converted to TreeMix format using a

237   custom Python script. A total of 71 out of 74 markers met our criteria, resulting in a matrix of

238   355 SNPs (dataset 4). TreeMix was invoked with –k 5 to account for linkage disequilibrium

239   for SNPs from the same marker. In consecutive analyses, we added from one to three

240   migration edges to allow for gene flow in the tree. We also ran TreeMix with an alternative

241   dataset using only 1 SNP per marker with the highest MAF.

242   2.5 Gene flow among OTUs

243   We first summarized the pattern of shared variation in our dataset by counting the numbers of

244   shared haplotypes between OTUs in a custom Python script using dataset 2. We also used this

245   dataset to calculate d_{xy} values among the newt OTUs in DnaSP v5 (Librado and Rozas, 2009).

246   We estimated gene flow between all pairs of OTUs (36 pairwise comparisons) in an

247   Approximate Bayesian Computation (ABC) framework. We followed Zieliński et al. (2016)

248   in removing all fully coding markers from analyses, excluding all missing data by removing

249   loci or individuals in pairwise comparisons and excluding all admixed individuals; final

250   datasets included 60-66 loci with between 5 and 24 sequences per taxon (Table S3). The

251   information present in the data was summarized for each pairwise comparison with a set of 9

252   summary statistics (Table S3 and Extended Methods).

253   We tested four simple scenarios of pairwise species divergence and the extent and

254   timing of interspecific gene flow: i) a no gene flow (NGF) model in which an ancestral

255   population splits into two at time T_{SPLIT} with no genetic exchange between descendant

256   populations, ii) an admixture (ADM) model in which a fraction of genes is moved

257   instantaneously from one population to the other; this can occur once independently in each

258   direction at any time after divergence, iii) a constant gene flow (CGF) model in which gene

259   flow is continuous and bidirectional between descendent taxa after T_{SPLIT}, and iv) a recent

260   gene flow (RGF) model in which continuous and bidirectional gene flow between descendent

261   taxa was constrained to have occurred in the last 200,000 years (approximately 50,000 newt

262   generations).

263   Coalescent simulations were done in fastsimcoal2.01 (Excoffier et al., 2013), and the

264   ABC analysis was conducted within the ABCtoolbox (Wegmann et al., 2010); detailed prior

265   and parameter values are given in the Extended Methods. A total of 10^6 datasets were

266   simulated under each demographic model from which we retained 1% (10^4) best simulations

267   and computed the marginal likelihood of the observed and retained datasets under the

268   generalized linear model (Leuenberger and Wegmann, 2010). To control the type I error for

269   multiple comparisons, we used a Bonferroni correction and removed models with the nominal

270    $P<0.0125$. The best fitting model was then selected via Bayes factors.

271   We estimated the power to distinguish between the four models within the ABC

272   framework by randomly picking 1000 pseudo-observed datasets from all simulations

273   generated for each model and checking how often the ABC procedure correctly predicted the

274   true model (the one that produced the dataset). Each pseudo-observed dataset was treated as

275   the observed data and used to calculate marginal densities of all compared models; Bayes

276   factors were used to select the best model. Because identical prior distributions were used for

277   all pairwise comparisons, we conducted a single power analysis using populations with the

278   fewest sequences (*L. kosswigi - L. v. meridionalis*). This can be considered the minimum

279   estimate as all other comparisons (with larger sample sizes) will have more power in

280   distinguishing between models.

281   Next, we formally tested whether the sharing of mtDNA haplotypes among *Lissotriton*

282   groups could be accounted for by ILS (incomplete lineage sorting) or is due to hybridization.

283   We assumed that the partially resolved nuclear phylogeny based on the concordant signal

284   from concatenated/BUCKy/TreeMix analyses (further referred to as the species tree) reflects

285   true relationships among the evolutionary lineages within *L. montandoni*/*L. vulgaris* and

286   followed the statistical approach of Joyce et al. (2011). If mtDNA similarities among

287   evolutionary lineages result from ILS, then mtDNA sequences simulated within the true

288   species tree should replicate the observed mtDNA data. If mtDNA introgression has occurred,

289   sequences simulated on alternative species trees, assuming closest relationships between the

290   lineages showing highest mtDNA similarity, should better reproduce the observed data.

291   Because the relationships between the evolutionary lineages have not been resolved

292   completely, both tests were based on four lineages with relationships well-supported by

293   nuclear data: i) N *L. v. vulgaris*, *L. v. ampelensis*, *L. kosswigi* and *L. montandoni*; ii) S *L. v.*

294   *vulgaris*, *L. v. meridionalis*, *L. schmidtleri* and *L. graecus* (Fig. 2). For *L. montandoni* two

295   scenarios were evaluated, allowing introgression from either *L. v. ampelensis* or N *L. v.*

296   *vulgaris*. For each evolutionary lineage we randomly sampled one sequence from each

297   locality for which mtDNA sequences were available (Babik et al., 2005; Pabijan et al., 2015;

298   Zieliński et al., 2013). These sequences were used to calculate parameters (times of

299   divergence and mutation-scaled effective population sizes of extant and ancestral taxa) of

300   competing species trees in BPP v3.1. A thousand gene trees were simulated for each species

301   tree with MCcoal. Sequences were simulated along gene trees using SeqGen (Rambaut and

302   Grass, 1997) assuming the HKA + gamma model of sequence evolution with parameter

303   values estimated in MEGA6 (Tamura et al., 2013). For each scenario mean and minimum

304   uncorrected (p) distances between evolutionary lineages were calculated for 1000 simulated

305   datasets and compared to the observed distances to obtain *P* values for individual

306   comparisons. *P* values from individual tests were combined using Fisher's method.

307   2.6 Data archiving

308 Input data and custom scripts used for data transformation and analysis are available in Dryad

309 digital repository with doi:[to be submitted upon manuscript acceptance]. DNA sequence

310 alignments for all markers were submitted to GenBank: accession nos. [to be submitted upon

311 manuscript acceptance]. Additional analyses are provided as Supplementary Data.

312 **3. Results**

313 The largest dataset 1 contained 128 individuals and 74 loci with an average of 72.1 ± 20.29

314 haplotypes/locus (range 29-117) and 1.9 ± 3.87 % missing data per locus. Markers were of

315 similar length (498.9 ± 6.79 bp) and highly polymorphic with an average of 91.8 ± 34.56

316 segregating sites per marker, one third of these (29.1 ± 9.52) were singleton polymorphisms

317 (Table S4).

318 3.1 Species delimitation

319 Bayesian clustering solutions at $K \leq 6$ had low probabilities. $Pr(K)$ plateaued at $K = 7$ (Fig.

320 S2) and therefore we further only considered analyses at $K = 7\text{-}12$ (60 analyses in total). Most

321 of these 60 analyses contained clusters that grouped all individuals of a given subspecies or

322 species together (Fig. 1B, Table S5). The top ten analyses with highest lnP all contained $K = 9$

323 groups with identical arrangements of individuals in clusters. Analyses with $K > 9$ contained

324 at least one cluster that was assigned zero or trivial fractions of the data, indicating that under

325 high K values, the number of meaningful clusters was lower than the assumed K. We thus

326 inferred 9 clusters with high certainty (Fig. 1B, Table S5). Five of these clusters correspond to

327 morphologically designated species or subspecies: *L. montandoni*, *L. graecus*, *L. v.*

328 *meridionalis*, *L. kosswigi* and *L. lantzi*. The nominal subspecies was subdivided into two

329 clusters that we designate North *L. v. vulgaris* (N *L. v. vulgaris*) and South *L. v. vulgaris* (S *L.*

330 *v. vulgaris*), with the former living predominantly to the north and east of the Carpathian arc

331 and the latter to the west and south of the Danube. The genetic cluster encompassing *L.*

15

332   *schmidtleri*, a taxon described from western Anatolia that is morphologically similar to the

333   nominal subspecies, was also found in the southeastern Balkans. The genetic cluster including

334   *L. v. ampelensis* contained four individuals from eastern Slovakia, extreme western Ukraine

335   and Romania classified as *L. v. vulgaris* according to morphology. Following Rosenberg et al.

336   (2001), we consider that the frequency with which each taxon formed an exclusive cluster

337   over all 60 analyses is a reliable measure of its support (Table S5). This ranged from 70% in

338   *L. kosswigi* to 88% in *L. graecus* and *L. schmidtleri* and considerably exceeded the frequency

339   with which particular taxa clustered together or were split into two or more groups. Some

340   evidence of additional substructure was found in South *L. v. vulgaris* and *L. graecus* (Fig. S3).

341   Admixture was consistently detected in nine individuals (7.0%; Fig. 1B, see Table S1

342   for estimated admixture proportions), five of which originated from the western part of the

343   range of *L. vulgaris* (admixed N *L. v. vulgaris*/S *L. v. vulgaris*, morphologically classified as

344   *L. v. vulgaris*), a single individual from northern Serbia (*L. v. ampelensis*/S *L. v. vulgaris,*

345   morphological *L. v. vulgaris*), one from Kosovo (S *L. v. vulgaris/L. graecus*, morphologically

346   undetermined), and two morphologically undetermined newts from the Romanian Carpathians

347   composed of two (N *L. v. vulgaris/L. v. ampelensis*) or three (N *L. v. vulgaris/L. v.*

348   *ampelensis*/*L. montandoni*) genetic clusters.

349   We conducted joint inference of species delimitation and phylogeny using BPP 3 with

350   the nine OTUs defined in STRUCTURE. The posterior probabilities of each of these equaled

351   1.00 in all analyses under a wide range of priors and different starting trees (Table 1). All

352   models in the 95% credibility sets contained the nine OTUs. The multispecies coalescent

353   model in BPP recovered a number of different species trees under the applied parameter

354   settings (Table 1); their topologies and posterior probabilities varied depending on the prior

355   specification, and to a limited extent, on seed number. Although the latter may suggest a lack

356   of convergence, species trees with highest support were mostly congruent across analyses.

357   Notably, *L. montandoni* and *L. v. ampelensis* were consistently recovered as sister taxa.

358   We used the gene trees calculated in MrBayes to estimate the genealogical exclusivity

359   of each candidate species. Typically, each genealogy in the post-burnin posteriors had a

360   different topology. This was expected because there was limited phylogenetic information

361   contained within each marker and many tips (257 including outgroup) in the trees.

362   Unsurprisingly, consensus gene trees calculated for each marker were mostly unresolved, and

363   showed high levels of discordance (data not shown). Nonetheless, the majority of the

364   genealogies showed a nonrandom clustering pattern for the delimited *Lissotriton* groups as

365   indicated by the highly significant *egsi* (Table 2). We inferred high exclusivity for *L. kosswigi*

366   and *L. lantzi* and with about 40% of genes monophyletic, and moderate *egsi* values for *L.*

367   *graecus*, *L. montandoni*, *L. schmidtleri* and *L. v. meridionalis*. The values of *egsi* were

368   relatively low but still highly significant for *L. v. ampelensis*, S *L. v. vulgaris* and N *L. v.*

369   *vulgaris*.

370   3.2 Phylogenetic results

371   In concatenation analyses, we found that the individuals within OTUs always formed clades

372   with posterior probabilities (PP) of 1.0, we therefore collapsed individuals into groups and

373   show a consensus tree over all replicates (Fig. 2A) and separately for each of the 10

374   concatenation replicates (Fig. S4). The positions of some clades were consistent across all

375   replicates and were always fully supported (PP = 1.0). These included the basal placement of

376   *L. montandoni,* the subsequent split of clade 1 composed of *L. graecus* and *L. kosswigi*, and

377   the sister group relationship of *L. v. meridionalis* and S *L. v. vulgaris*. Moreover, the

378   concatenated analyses invariably identified clade 2 composed of *L. lantzi*, *L. schmidtleri*, S *L.*

379   *v. vulgaris*, N *L. v. vulgaris*, *L. v. ampelensis* and *L. v. meridionalis*. Our replicate analyses

17

380   differed in the choice of sequences at heterozygous loci during the concatenation process; the

381   results show that this influenced the branching patterns of the concatenated phylogenetic

382   analyses by altering the positions of 4 taxa within clade 2 (*L. lantzi*, *L. schmidtleri*, N *L. v.*

383   *vulgaris* and *L. v. ampelensis*). Nearly all alternative arrangements were strongly supported in

384   one or more concatenation replicates (Fig. S4).

385   A consensus of the 50 replicate primary concordance trees from BUCKy (Fig. 2B)

386   shows that all *L. vulgaris* taxa grouped together (to the exclusion of *L. montandoni*) across all

387   replicates. The mean concordance factor represented by the mean number of genes supporting

388   this clade was 20.5 ± 2.2 out of a total of 70 genes. Clades 1 and 2 as well as the sister group

389   relationship between S *L. v. vulgaris* and *L. v. meridionalis* were relatively well-supported,

390   although concordance factors were generally low (on average <15 genes), suggesting that

391   more than one tree may equally well describe the history of these taxa. We examined this

392   issue by extracting concordance factors from each replicate BUCKy analysis for clades with

393   relatively high support (mostly encompassing those with two terminal taxa, Fig. S5). Primary

394   histories were well-discernible in the cases of *L. montandoni*, *L. v. meridionalis*, S *L. v.*

395   *vulgaris*, *L. lantzi*, *L. graecus* and *L. kosswigi*. However, between 3 and 6 primary histories

396   could be discerned for N *L. v. vulgaris*, *L. v. ampelensis* and *L. schmidtleri*, shown by similar

397   mean concordance factors and largely overlapping quartiles (Fig. S5).

398   The maximum likelihood topologies recovered by TreeMix based on 1 or 5 SNPs per

399   marker (Fig. 2C) were very similar to the consensus topology of the concatenated analysis

400   (Fig. 2A). After adding migration edges, we recovered gene flow between *L. v. ampelensis*

401   and *L. montandoni*, followed by gene flow of lesser magnitude between *L. graecus* and *L.*

402   *schmidtleri* and the ancestor of S *L. v. vulgaris* and *L. v. meridionalis* (Fig. 2D and Fig. S6).

403   3.3 Gene flow among lineages

18

404   We found a gradient in divergence values (d_{xy}) among newt OTUs ranging between 1.14-

405   1.59% (Fig. 3, Table S6). Each pair of OTUs shared haplotypes at some markers (Fig. 3),

406   although in many cases this amounted to less than 2% and may be indicative of retained

407   ancestral variation. The highest proportions were shared between N *L. v. vulgaris* and *L. v.*

408   *ampelensis* (9.1%), *L. montandoni* and two other lineages (7.5 and 6.7% for N *L. v. vulgaris-*

409   *L. montandoni* and *L. v. ampelensis-L. montandoni*, respectively) and three pairs involving S

410   *L. v. vulgaris* and neighboring clades *L. v. ampelensis*, N *L. v. vulgaris* and *L. v. meridionalis*

411   (5.2, 4.6 and 3.3%, respectively). We note that all instances of relatively high levels of

412   haplotype sharing were inferred for Central European taxa that at present occur parapatrically.

413   In most pairwise comparisons of OTUs within the ABC framework at least one model

414   could reproduce the observed data (Tables S7 and S8). The analyses had good power to

415   discriminate between the four models (Table S8). Posterior probabilities for models varied

416   considerably among pairwise taxa comparisons (Fig. 4A) with a clear predominance of the

417   admixture (ADM) model and only 6 comparisons in which recent (in the last 200 kya) or

418   continuous gene flow prevailed, all confined to currently parapatric, Central European

419   lineages. However, in other cases episodes of gene flow in the ADM model were timed to

420   have occurred deep in the past (e.g. modal values for posteriors >1 Ma), making ADM and

421   NGF equivalent in the sense of ruling out recent and constant gene flow (e.g. in *L. kosswigi-L.*

422   *v. meridionalis, L. kosswigi-L. graecus, L. kosswigi-L. lantzi, L. montandoni-L. lantzi, L.*

423   *montandoni*-S *L. v. vulgaris*; Table S9). In other pairwise comparisons modal values for

424   admixture times in the ADM model were inferred to have occurred relatively recently, close

425   to the upper limit of the prior (e.g. *L. montandoni-L. v. ampelensis*, N *L. v. vulgaris-L.*

426   *kosswigi*), making the ADM and RGF models comparable. However, the posterior

427   distributions for the admixture time parameters were in general very broad, indicating that

428   data were not very informative in dating admixture events.

429   Phylogenies estimated from mtDNA under the assumption of ILS substantially

430   differed from trees estimated assuming mtDNA introgression (i.e. the topology was

431   incongruent with the species tree based on nuclear data, Fig. 5). Under ILS entire trees and

432   internal branches were both very short. Minimum mtDNA divergence between lineages

433   readily distinguished between ILS and hybridization. For both *L. montandoni* and *L. graecus*,

434   scenarios assuming hybridization fit the data well and were strongly preferred over ILS

435   (Table 3). One of the two hybridization scenarios involving *L. montandoni* fit the data better

436   than the other, although both hybridization scenarios had much better fit than ILS. Apparently

437   the scenario assuming introgression between N *L. v. vulgaris* and *L. montandoni* received

438   higher support because of more extensive mtDNA haplotype sharing between these two than

439   between *L. montandoni* and *L. v. ampelensis*. Mean mtDNA divergence between lineages was

440   not informative in distinguishing between ILS and hybridization as both scenarios generated

441   mean divergence that was not significantly different from the observed values (data not

442   shown).

443   **4. Discussion**

444   This study documents a series of lineages representing a continuum of genetic divergence

445   with ample evidence for historical contact and gene flow between lineages. We demonstrate

446   the importance of geographic conditions (allopatry vs. parapatry) and historical contingencies

447   such as time since divergence and timing of secondary contact in determining the continuum

448   of divergence that can be quantified in the present. Moreover, we show that a combination of

449   population genetic and phylogenetic approaches is required to describe and measure this

450   continuum. In the following sections we discuss our findings for *Lissotriton* newts, their more

451   general implications and outline research areas where methodological advances are needed.

452   4.1 Robust delimitation despite substantial gene flow

453 All applied delimitation methods, based on allele frequencies, multispecies coalescent and

454 genealogical concordance, robustly delimited nine evolutionary lineages. Some of these

455 lineages correspond to described morphological subspecies, while others are morphologically

456 cryptic (N *L. v. vulgaris*, S *L. v. vulgaris*) or include two distinct morphologies (*L. v.*

457 *ampelensis*). This result is not an artifact of limited sampling under isolation by distance,

458 because admixed individuals are rare and boundaries between lineages in well-sampled areas

459 are sharp. The delimited entities are distinguishable in both allele frequency-based and

460 genealogical frameworks, but are at various stages of divergence (Fig. 3). Substantial

461 admixture between N *L. v. vulgaris* and S *L. v. vulgaris* in the postglacial expansion area in

462 western Europe indicates that some lineages retain considerable potential for genetic

463 exchange. We found evidence for recent gene flow between five other lineage pairs, all of

464 which occur parapatrically in Central Europe (Figs 1 and 4b; see Zieliński et al., 2016, for a

465 detailed assessment of genetic exchange between *L. montandoni* and two *L. vulgaris*

466 lineages). Moreover, episodes of gene flow between lineages in the more distant past may

467 have been commonplace, given the overall weak support for the divergence with no gene flow

468 model in the ABC analyses (Fig. 4), two cases of confirmed old mtDNA introgression (Table

469 3), and several other instances of mtDNA paraphyly (Babik et al., 2005; Nadachowska and

470 Babik, 2009; Pabijan et al., 2015). Thus, it is by no means certain that all delimited newt

471 lineages will continue to evolve independently. The newt system is a good example of a

472 broader phenomenon: as reproductive isolation progresses, the incipient species experience a

473 prolonged phase of parapatric/allopatric structured populations which may episodically

474 exchange genes. In some instances, secondary contact may lead to the fusion of non-sister

475 lineages over parts of their collective range (e.g. N *L. v. vulgaris* and S *L. v. vulgaris* in

476 western Europe). This interpretation is in line with recent genetic and molecular studies of

477 speciation showing that post-divergence gene flow is common, e.g. it was an important

478   feature of hominin history (Pääbo, 2015), and sometimes occurs at high levels (e.g. Muir et

479   al., 2012; Nevado et al., 2011; Osborne et al., 2016; Sun et al., 2012).

480   4.2 Newt phylogeny and evolution of male nuptial morphology

481   The species tree of the *L. vulgaris* group could not be fully resolved (Fig. 2A). Relationships

482   that received high support included *L. montandoni* as the outgroup to all *L. vulgaris* taxa, *L.*

483   *graecus* and *L. kosswigi* (clade 1) as the sister group to other *L. vulgaris* lineages (clade 2),

484   and the sister group relationship between S *L. v. vulgaris* + *L. v. meridionalis*. Although the

485   monophyly of clade 2 is supported, the relationships among OTUs within this group are

486   uncertain. However, we acknowledge that only one (TreeMix) of the four applied

487   phylogenetic methods specifically modelled gene flow among OTUs. Nonetheless, well-

488   supported nodes in the concatenation and concordance analyses were compatible with the

489   topology of the maximum likelihood tree from TreeMix, suggesting that gene flow among

490   OTUs did not overwhelm the phylogenetic signal over all parts of the tree. However, species

491   tree estimation in BPP under the multispecies coalescent consistently recovered a sister group

492   relationship between *L. montandoni* and *L. v. ampelensis* (Table 1). Likewise, analyses using

493   *BEAST (Heled and Drummond, 2010), which experienced overall convergence issues,

494   produced similar results (data not shown). Given the strong evidence for recent gene flow

495   among these two taxa (Fig. 4; Zieliński et al., 2016), we consider this relationship as highly

496   unlikely. Coalescent-based species tree methods are sensitive to violations of the assumption

497   of no gene flow, particularly between non-sister taxa (Leaché et al., 2013; Solís-Lemus and

498   Ané, 2016), and are thus unsuited to study the relationships within the *L. vulgaris* complex.

499   Given the increasing number of studies reporting reticulate evolution, there is an urgent need

500   for progress in methods co-estimating phylogeny and gene flow in multispecies and

501   multilocus datasets; phylogenetic multilocus network methods (Solís-Lemus and Ané, 2016;

502   Yu et al., 2013, 2014) appear promising in this respect.

503   The species tree for the *L. vulgaris* group nonetheless sheds light on morphological

504   evolution in newts. The male nuptial morphology of *L. montandoni* consists of a smooth and

505   low crest, prominent tail filament and dorso-lateral ridges. Similar male morphologies are also

506   present in the more distantly related *L. helveticus*, *L. italicus* and *L. boscai*. This particular

507   suite of phenotypic traits may be an adaptation for the effective transmission of waterborne

508   pheromones (Pecio and Rafiński, 1985) and could signify the predominance of olfactory cues

509   for species recognition (Secondi et al., 2005). On the other hand, the derived condition of

510   prominent crests and overall larger male body size in most *L. vulgaris* lineages indicates a

511   shift towards visual cues (Secondi et al., 2012), although other explanations are possible such

512   as divergence in female preference for larger male body size (Haerty et al., 2007; Secondi et

513   al., 2010). Whatever the underlying cause(s), our species phylogeny shows that *montandoni-*

514   like male morphology was present in the ancestral *L. vulgaris* population, conserved in the *L.*

515   *graecus*/*L. kosswigi* clade, and replaced by the derived morphology in the sister clade giving

516   rise to other extant *L. vulgaris* lineages. The intermediate breeding male morphologies of *L. v.*

517   *ampelensis* and *L. v. meridionalis* (Raxworthy, 1990) could be interpreted as independent,

518   partial reversions to the ancestral morphology due to convergent evolution. Alternatively, and

519   possibly more likely given the evidence for substantial gene flow from neighboring taxa,

520   these intermediate morphologies could be the result of an influx of genes underlying the

521   derived morphology and dilution of *montandoni*-like ancestral traits. These two hypotheses

522   could be tested with genome-wide data.

523   4.3 Isolation and gene flow revealed by ABC modeling

524   Recognizing the limitations of existing methodologies, we explored gene flow between pairs

525   of taxa in a model-based framework using Approximate Bayesian Computation (ABC). This

526   approach, although quite simple, has been effective in unraveling the process of gene flow in

527   the newt system. The data had good power in distinguishing among the four scenarios of gene

528   flow and provided quantitative measures of support for the various models. However,

529   analyses modeling gene flow between two populations without incorporation of additional

530   populations have been criticized because ignoring such "ghost" populations may affect

531   parameter estimates or even model choice (Beerli, 2004; Eaton et al., 2015; Slatkin, 2005;

532   Strasburg and Rieseberg, 2010). We note though that pairwise comparisons among all extant

533   taxa may partially alleviate this issue. The availability of all pairwise comparisons allows the

534   identification and reinterpretation of problematic cases, such as support for recent gene flow

535   between allopatric taxa which have not likely been in recent contact, but which both may have

536   exchanged genes with other populations. In our case, inferences were largely consistent with

537   the geographic distributions of the lineages (parapatry vs. allopatry) and we accept them as

538   working hypotheses. In general, given the current state of the field, the use of simple pairwise

539   models in complexes of interbreeding species may be useful because they offer a feasible way

540   of distinguishing among different scenarios of gene flow and building more complex, but still

541   testable, hypotheses.

542   In addition to model selection, ABC estimates demographic parameters which

543   facilitate the interpretation of evolutionary history along the speciation continuum. Estimates

544   of long-term, coalescent effective population sizes (N_e) for the *Lissotriton* lineages are quite

545   large, ranging roughly between 80,000 and 800,000 (Table S9). Independent assessments

546   place the divergence time of *L. montandoni* and *L. vulgaris* between 3.7 to 6.3 mya (Stuglik

547   and Babik, 2016), while mtDNA lineages within *L. vulgaris* split in close succession during

548   the late Pliocene and early Pleistocene (Babik et al., 2005; Pabijan et al., 2015). This

549   timeframe suggests that most *Lissotriton* lineages have not attained the $4N_e$ generations when

550   roughly half of the loci in the genome achieve reciprocal monophyly (Hudson and Coyne,

551   2002; Degnan and Rosenberg, 2009), thus widespread incomplete lineage sorting (Table 2)

552   and the presence of identical haplotypes amongst all lineage pairs are expected (Fig. 3).

553 However, the lineages exchanging genes most extensively (*L. v. ampelensis*, N *L. v. vulgaris*,

554 S *L. v. vulgaris, L. v. meridionalis*) also have the largest N_e's (Fig. 4B, Table S9). This

555 suggests that post-divergence gene flow contributed to elevated N_e estimates, although long-

556 term population structure within lineages may also inflate N_e. We postulate that the existence

557 of a transitional phase, in which differentiated lineages exchange genes, may explain or

558 contribute to the large ancestral population sizes inferred by various methods (IM, ABC,

559 PSMC) in many species (e.g. Duvaux et al., 2011; Nadachowska-Brzyska et al., 2015; Won et

560 al., 2005).

561 4.4 Introgression explains mtDNA paraphyly

562 With a partially resolved phylogeny, we were able to test statistically for mtDNA

563 introgression suggested previously (Babik et al., 2005; Nadachowska and Babik, 2009;

564 Pabijan et al., 2015). We confirmed introgression in two of the most striking cases (from N *L.*

565 *v. vulgaris* into *L. montandoni* and S *L. v. vulgaris* into *L. graecus*), effectively explaining the

566 discordance between mtDNA, nuclear genes and morphology, and attributing it to extensive

567 recent and ancient mtDNA introgression. While there is evidence that it has been

568 accompanied by introgression of nuclear genes in the case of *L. montandoni*, we do not have

569 strong evidence of nuclear introgression into *L. graecus*. Better power to reconstruct the

570 extent and timing of nuclear introgression would be obtained with a larger amount of data,

571 particularly from longer genomic regions to explore information contained in haplotype

572 spectra (Harris and Nielsen, 2013).

573 4.5 Taxonomic implications

574 We note that the application of a rigid taxonomy in which we appropriate scientific names to

575 all nine genetically distinct lineages delimited herein would not fully capture the intricacies of

576 the evolutionary history of *Lissotriton* newts. As stated previously (Wiens, 2007), the

577   delimitation of species poses the problem of thresholding the continuous processes of

578   speciation and lineage amalgamation. Although a number of authors have recognized some of

579   the morphological *L. vulgaris* subspecies as full species (e.g. Dubois and Raffaëlli, 2009;

580   Frost, 2016; Skorinov et al*.,* 2014; Wielstra et al*.*, 2015), these relegations were not based on

581   new data but on inconclusive mtDNA variation, geographic range limits, and morphology.

582   We delimited four distinct southern taxa for which our data strongly suggest species

583   status: *L. v. graecus* as *L. graecus* (Wolterstorff, 1906), *L. v. kosswigi* as *L. kosswigi*

584   (Freytag, 1955), *L. v. lantzi* as *L. lantzi* (Wolterstorff, 1914) and *L. v. schmidtleri* as *L.*

585   *schmidtleri* (Raxworthy, 1988) *L. v.* [and not *L. schmidtlerorum*, see Dubois (2007) and

586   Dubois and Raffaëlli (2009)]. We base this assertion on the concordant signals of divergence

587   and independence from allele frequency- and genealogy-based delimitation methods,

588   genealogical sorting, a nearly complete lack of hybrids in well-sampled areas and little

589   evidence for genetic exchange in the recent past. Moreover, *L. kosswigi* and *L. lantzi* are

590   allopatrically distributed (Skorinov et al., 2014; Wielstra et al*.*, 2015), making gene exchange

591   with other lineages improbable in the near future. More extensive sampling in Bulgaria and

592   eastern Greece is needed to characterize the contact between L. schmidtleri and other smooth

593   newt lineages. On the other hand, four central European *L. vulgaris* lineages are

594   interconnected by nontrivial amounts of gene flow. These taxa show fusion following range

595   expansion in the morphologically cryptic N *L. v. vulgaris* and S *L. v. vulgaris*, extensive

596   genetic exchange with neighboring lineages in *L. v. ampelensis*, and continuous gene flow

597   since divergence between *L. v. meridionalis* and S *L. v. vulgaris*. These results suggest that we

598   may be observing the loss of incipient divergence through hybridization in these taxa.

599   4.6 Conclusions

600   We found that *Lissotriton* newts represent a continuum of genetic divergence with varying

601   levels of shared genetic variation among taxon pairs. This pattern invokes long-term isolation

602   and independent evolution in four southern smooth newt species, genetic exchange across

603   parapatric borders for several taxa in Central Europe, and effective fusion of previously

604   separated gene pools of two lineages in the post-glacial expansion areas of Western Europe.

605   The profound discordance between taxonomic boundaries and mtDNA in *Lissotriton* is

606   explained by extensive mtDNA introgression rather than by other processes. These features

607   make the *L. vulgaris* species group a suitable system to examine the fission/fusion dynamics

608   of the speciation continuum. The newt system is relevant because many species may have

609   experienced such long-term structured populations. However, we also highlight that better

610   methods, jointly modeling incomplete lineage sorting and gene flow, are needed to analyze

611   such systems.

612   **Acknowledgements**

618

References

Ané, C., Larget, B., Baum, D.A., Smith, S.D., Rokas, A., 2007. Bayesian estimation of concordance among gene trees. Mol. Biol. Evol. 24, 412–426.

Babik, W., Rafiński, J., 2004. Relationship between morphometric and genetic variation in pure and hybrid populations of the smooth and Montandon's newt (*Triturus vulgaris* and *T. montandoni*). J. Zool. 262, 135–143.

Babik, W., Szymura, J.M., Rafiński, J., 2003. Nuclear markers, mitochondrial DNA and male secondary sexual traits variation in a newt hybrid zone (*Triturus vulgaris*×*T. montandoni*). Mol. Ecol. 12, 1913–1930.

Babik, W., Branicki, W., Crnobrnja-Isailović, J., Cogălniceanu, D., Sas, I., Olgun, K., Poyarkov, N.A., Garcia-París, M., Arntzen, J.W., 2005. Phylogeography of two European newt species—discordance between mtDNA and morphology. Mol. Ecol. 14, 2475–2491.

Beerli, P., 2004. Effect of unsampled populations on the estimation of population sizes and migration rates between sampled populations. Mol. Ecol. 13, 827–836.

Bour, R., Bringsøe, H., Vanderhaege, M., 2002. *Triturus vulgaris* (Linnaeus, 1758) at its southern limit: distribution on the Peloponnese, Greece, with range extensions from the Central and South Peloponnese. Alytes 20, 67–76.

Bousbouras, D., Ioannidis, Y., 1997. The distribution and habitat preferences of the amphibians of Prespa National Park, in: Crivelli, A.J., Catsadorakis, G. (Eds.), Lake Prespa, Northwestern Greece. A Unique Balkan Wetland. Springer, the Netherlands, pp. 127–133.

Coyne, J.A., Orr, H.A, 2004. Speciation. Sinauer Associates, Sunderland, MA.

Cruickshank, T.E., Hahn, M.W., 2014. Reanalysis suggests that genomic islands of speciation are due to reduced diversity, not reduced gene flow. Mol. Ecol. 23, 3133–3157.

Cummings, M.P., Neel, M.C., Shaw, K.L., 2008. A genealogical approach to quantifying

644   lineage divergence. Evolution 62, 2411–2422.

645   Darriba, D., Taboada, G.L., Doallo, R., Posada, D. 2012. jModelTest 2: more models, new

646   heuristics and parallel computing. Nat. Methods 9, 772–772.

647   Degnan, J.H., Rosenberg, N.A., 2009. Gene tree discordance, phylogenetic inference and the

648   multispecies coalescent. Trends Ecol. Evol. 24, 332–340.

649   de Queiroz, K., 2007. Species concepts and species delimitation. Syst. Biol. 56, 879–886.

650   Dubois, A., 2007. Genitives of species and subspecies nomina derived from personal names

651   should not be emended. Zootaxa 1550, 49–68.

652   Dubois, A., Raffaëlli, J., 2009. A new ergotaxonomy of the family Salamandridae Goldfuss,

653   1820 (Amphibia, Urodela). Alytes 26, 1–85.

654   Duvaux, L., Belkhir, K., Boulesteix, M., Boursot, P., 2011. Isolation and gene flow: inferring

655   the speciation history of European house mice. Mol. Ecol. 20, 5248–5264.

656   Earl, D.A., vonHoldt, B.M., 2012. STRUCTURE HARVESTER: a website and program for

657   visualizing STRUCTURE output and implementing the Evanno method. Conserv. Genet.

658   Resour. 4, 359–361.

659   Eaton, D.A., Hipp, A.L., González-Rodríguez, A., Cavender-Bares, J, 2015. Historical

660   introgression among the American live oaks and the comparative nature of tests for

661   introgression. Evolution 69, 2587–2601.

662   Excoffier, L., Dupanloup, I., Huerta-Sánchez, E., Sousa, V.C., Foll, M., 2013. Robust

663   demographic inference from genomic and SNP data. PLoS Genet. 9, e1003905.

664   Frost, D.R., 2016. Amphibian Species of the World 6.0, an Online reference. Available at

665   http://research.amnh.org/vz/herpetology/amphibia. Accessed December 20, 2016.

666   Harris, K., Nielsen, R., 2013. Inferring demographic history from a spectrum of shared

667   haplotype lengths. PLoS Genet. 9, e1003521.

668   Haerty, W., Gentilhomme, E., Secondi, J., 2007. Female preference for a male sexual trait

669   uncorrelated with male body size in the palmate newt (*Triturus helveticus*). Behaviour 144,

670   797–814.

671   Heled, J., Drummond, A.J., 2010. Bayesian inference of species trees from multilocus data.

672   Mol. Biol. Evol. 27, 570–580.

673   Huang, J-P., Knowles, L.L., 2016. The species versus subspecies conundrum: quantitative

674   delimitation from integrating multiple data types within a single Bayesian approach in

675   Hercules beetles. Syst. Biol. 65, 685–699.

676   Hudson, R.R., Coyne, J.A., 2002. Mathematical consequences of the genealogical species

677   concept. Evolution 56, 1557–1565.

678   Joyce, D.A., Lunt, D.H., Genner, M.J., Turner, J.F., Bills, R., Seehausen, O., 2011. Repeated

679   colonization and hybridization in Lake Malawi cichlids. Curr. Biol. 21, R108–R109.

680   Kotlík, P., Zavadil, V., 1999. Natural hybrids between the newts *Triturus montandoni* and *T.*

681   *vulgaris*: morphological and allozyme data evidence of recombination between parental

682   genomes. Folia Zool. 48, 211–218.

683   Kopelman, N.M., Mayzel, J., Jakobsson, M., Rosenberg, N.A., Mayrose, I., 2015. Clumpak: a

684   program for identifying clustering modes and packaging population structure inferences

685   across K. Mol. Ecol. Resour. 15, 1179–1191.

686   Krizmanic, I., Mesaroš, G., Džukic, G., Kalezic, M.L., 1997. Morphology of the smooth newt

687   (*Triturus vulgaris*) in former Yugoslavia: taxonomical implications and distribution

688   patterns. Acta Zool. Acad. Sci. H. 43, 345–357.

689   Larget, B., Kotha, S.K., Dewey, C.N., Ané, C., 2010. BUCKy: Gene tree / species tree

690   reconciliation with the Bayesian concordance analysis. Bioinformatics 26, 2910–2911.

691   Leaché, A.D., Harris, R.B., Rannala, B., Yang, Z., 2014. The influence of gene flow on

692   species tree estimation: a simulation study. Syst. Biol. 63, 17–30.

693   Leuenberger, C., Wegmann, D., 2010. Bayesian computation and model selection without

694   likelihoods. Genetics 184, 243–252.

695   Librado, P., Rozas, J., 2009. DnaSP v5: A software for comprehensive analysis of DNA

696   polymorphism data. Bioinformatics 25, 1451–1452.

697   Macgregor, H.C., Sessions, S.K., Arntzen, J.W., 1990 An integrative analysis of phylogenetic

698   relationships among newts of the genus *Triturus* (family Salamandridae), using

699   comparative biochemistry, cytogenetics and reproductive interactions. J. Evol. Biol. 3,

700   329–373.

701   Michalak, P., Rafiński, J., 1999. Sexual isolation between two newt species, *Triturus vulgaris*

702   and *T. montandoni* (Amphibia, Urodela, Salamandridae). Biol. J. Linn. Soc. 67, 343–352.

703   Michalak, P., Grzesik, J., Rafiński, J., 1997. Tests for sexual incompatibility between two

704   newt species, *Triturus vulgaris* and *Triturus montandoni*: no-choice mating design.

705   Evolution 51, 2045–2050.

706   Miller, M.A., Pfeiffer, W., Schwartz, T., 2010. Creating the CIPRES Science Gateway for

707   inference of large phylogenetic trees. Proc. Gate. Comp. Environ. Work, 1–8.

708   Muir, G., Dixon, C.J., Harper, A.L., Filatov, D.A., 2012. Dynamics of drift, gene flow, and

709   selection during speciation in *Silene*. Evolution 66, 1447–1458.

710   Nadachowska, K., Babik, W., 2009 Divergence in the face of gene flow: the case of two

711   newts (Amphibia: Salamandridae). Mol. Biol. Evol. 26, 829–841.

712   Nadachowska-Brzyska, K., Li, C., Smeds, L., Zhang, G., Ellegren, H., 2015. Temporal

713   dynamics of avian populations during Pleistocene revealed by whole-genome sequences.

714   Curr. Biol. 25, 1375–1380.

715   Nevado, B., Fazalova, V., Backeljau, T., Hanssens, M., Verheyen, E., 2011. Repeated

716   unidirectional introgression of nuclear and mitochondrial DNA between four congeneric

717   Tanganyikan cichlids. Mol. Biol. Evol. 28, 2253–2267.

718   Nylander, J.A., Wilgenbusch, J.C., Warren, D.L., Swofford, D.L., 2008. AWTY (are we there

719   yet?): a system for graphical exploration of MCMC convergence in Bayesian

720   phylogenetics. Bioinformatics 24, 581–583.

721   Osborne, O., Chapman, M., Nevado, B., Filatov, D., 2016. Maintenance of species boundaries

722   despite ongoing gene flow in ragworts. Genome Biol. Evol. 8, 1038–1047.

723   Pabijan, M., Zieliński, P., Dudek, K., Chloupek, M., Sotiropoulos, K., Liana, M., Babik, W.,

724   2015. The dissection of a Pleistocene refugium: phylogeography of the smooth newt,

725   *Lissotriton vulgaris*, in the Balkans. J. Biogeogr. 42, 671–683.

726   Pääbo, S., 2015. The diverse origins of the human gene pool. Nat. Rev. Genet. 16, 313–314.

727   Pecio, A., Rafiński, J., 1985. Sexual behaviour of the Montandon's newt, *Triturus montandoni*

728   (Boulenger)(Caudata: Salamandridae). Amphibia-Reptilia 6, 11–22.

729   Petit, R.J., Excoffier, L., 2009. Gene flow and species delimitation. Trends Ecol. Evol. 24,

730   386–393.

731   Pickrell, J.K., Pritchard, J.K., 2012. Inference of population splits and mixtures from genome-

732   wide allele frequency data. PLoS Genet. 8, e1002967.

733   Pritchard, J.K., Stephens, M., Donnelly, P., 2000. Inference of population structure using

734   multilocus genotype data. Genetics 155, 945–959.

735   Rafiński, J., Arntzen, J.W., 1987. Biochemical systematics of the Old World newts, genus

736   *Triturus*: allozyme data. Herpetologica 43, 446–457.

737   Rambaut, A., Drummond, A.J., 2007. Tracer v1. 5. http://*tree.bio.ed.ac.uk/software/tracer*

738   Rambaut, A., Grass, N.C., 1997. Seq-Gen: an application for the Monte Carlo simulation of

739   DNA sequence evolution along phylogenetic trees. Comput. Appl. Biosci. 13, 235–238.

740   Rannala, B., Yang, Z., 2013. Improved reversible jump algorithms for Bayesian species

741   delimitation. Genetics 194, 245–253.

742   Raxworthy, C.J., 1990. A review of the smooth newt (*Triturus vulgaris*) subspecies, including

743   an identification key. Herpetol. J. 1, 481–492.

744   Rhymer, J.M., Simberloff, D., 1996. Extinction by hybridization and introgression. Annu.

745   Rev. Ecol. Syst. 27, 83–109.

746   Ronquist, F., Teslenko, M., van der Mark, P., Ayres, D.L., Darling, A., Höhna, S., Larget, B.,

747   Liu, L., Suchard, M.A., Huelsenbeck, J.P., 2012. MrBayes 3.2: efficient Bayesian

748   phylogenetic inference and model choice across a large model space. Syst. Biol. 61, 539–

749   542.

750   Rosenberg, N.A., Burke, T., Elo, K., Feldman, M.W., Freidlin, P.J., Groenen, M.A.M., Hillel,

751   J., Mäki-Tanila, A., Tixier-Boichard, M., Vignal, A., Wimmers, K., Weigend, S., 2001.

752   Empirical evaluation of genetic clustering methods using multilocus genotypes from 20

753   chicken breeds. Genetics 159, 699–713.

754   Rudman, S.M., Schluter, D., 2016. Ecological impacts of reverse speciation in threespine

755   stickleback. Curr. Biol. 26, 490–495.

756   Schmidtler, J.F., Franzen, M., 2004. *Triturus vulgaris* (Linnaeus, 1758)–Teichmolch, in:

757   Grossenbacher, K., Thiesemeier, B. (Eds.), Handbuch der Reptilien und Amphibien

758   Europas. Aula Verlag, Wiesbaden, Germany, pp. 847–967.

759   Schmidtler, J.J, Schmidtler, J.F., 1983. Verbreitung, Ökologie und unterartliche Gliederung

760   von *Triturus vulgaris* in der adriatischen Küstengebieten (Amphibia, Salamandridae).

761   Spixiana 6, 229–249.

762   Secondi, J., Haerty, W., Lodé, T., 2005. Female attraction to conspecific chemical cues in the

763   palmate newt *Triturus helveticus*. Ethology 111, 726–735.

764   Secondi, J., Johanet, A., Pays, O., Cazimajou, F., Djalout, Z., Lemaire, C., 2010. Olfactory

765   and visual species recognition in newts and their role in hybridization. Behaviour 147,

766   1693–1712.

767   Secondi, J., Lepetz, V., Théry, M., 2012. Male attractiveness is influenced by UV

768   wavelengths in a newt species but not in its close relative. PLoS One 7, e30391.

769   Skorinov, D.V., Kuranova, V.N., Borkin, L.J., Litvinchuk, S., 2008. Distribution and

770   conservation status of the Smooth Newt (*Lissotriton vulgaris*) in Western Siberia and

771   Kazakhstan. Russian J. Herpetol. 15, 157–165.

772   Skorinov, D., Doronin, I., Kidov, A., Tuniev, B., Litvinchuk, S., 2014. Distribution and

773   conservation status of the Caucasian newt, *Lissotriton lantzi* (Wolterstorff, 1914). Russian

774   J. Herpetol. 21, 251–268.

775   Slatkin, M., 1985. Gene flow in natural populations. Annu. Rev. Ecol. Syst. 16, 393–430.

776   Slatkin, M., 2005. Seeing ghosts: the effect of unsampled populations on migration rates

777   estimated for sampled populations. Mol. Ecol. 14, 67–73.

778   Solís-Lemus, C., Ané, C., 2016. Inferring phylogenetic networks with maximum

779   pseudolikelihood under incomplete lineage sorting. PLoS Genet. 12, e1005896.

780   Solís-Lemus, C., Yang, M., Ané, C., 2016. Inconsistency of species-tree methods under gene

781   flow. Syst. Biol. 65, 843–851.

782   Sousa, V., Hey, J., 2013. Understanding the origin of species with genome-scale data:

783   modelling gene flow. Nat. Rev. Genet. 14, 404–414.

784   Speybroeck, J., Beukema, W., Crochet, P-A., 2010. A tentative species list of the European

785   herpetofauna (Amphibia and Reptilia)–an update. Zootaxa 2492, 1–27.

786   Strasburg, J. L., Rieseberg, L.H., 2010. How robust are "isolation with migration" analyses to

787   violations of the IM model? A simulation study. Mol. Biol. Evol. 27, 297–310.

788   Stuglik, M.T., Babik, W., 2016. Genomic heterogeneity of historical gene flow between two

789   species of newts inferred from transcriptome data. Ecol. Evol. 6, 4513–4525.

790   Sun, Y., Corcoran, P., Menkis, A., Whittle, C.A., Andersson, S.G., Johannesson, H., 2012.

791   Large-scale introgression shapes the evolution of the mating-type chromosomes of the

792   filamentous ascomycete *Neurospora tetrasperma*. PLoS Genetics 8, e1002820.

793   Tamura, K., Stecher, G., Peterson, D., Filipski, A., Kumar, S., 2013. MEGA6: molecular

794   evolutionary genetics analysis version 6.0. Mol. Biol. Evol. 30, 2725–2729.

795   Wegmann, D., Leuenberger, C., Neuenschwander, S., Excoffier, L., 2010. ABCtoolbox: a

796   versatile toolkit for approximate Bayesian computations. BMC Bioinformatics 11, 116.

797   Wielstra, B., Bozkurt, E., Olgun, K., 2015. The distribution and taxonomy of *Lissotriton*

798   newts in Turkey (Amphibia, Salamandridae). ZooKeys 484, 11–23.

799   Wiens, J.J., 2007. Species delimitation: new approaches for discovering diversity. Syst. Biol.

800   56, 875–878.

801   Weisrock, D.W., Smith, S.D., Chan, L.M., Biebouw, K., Kappeler, P.M., Yoder, A.D., 2012.

802   Concatenation and concordance in the reconstruction of mouse lemur phylogeny: an

803   empirical demonstration of the effect of allele sampling in phylogenetics. Mol. Biol. Evol.

804   29, 1615–1630.

805   Wolf, J.B.W., Ellegren, H., 2016. Making sense of genomic islands of differentiation in light

806   of speciation. Nat. Rev. Genet. 18, 87–100.

807   Won, Y.J., Sivasundar, A., Wang, Y., Hey, J., 2005. On the origin of Lake Malawi cichlid

808   species: a population genetic analysis of divergence. P. Natl. Acad. Sci-Biol. 102, 6581–

809   6586.

810   Yang, Z., 2015. The BPP program for species tree estimation and species delimitation. Curr.

811   Zool. 61, 854–865.

812   Yang, Z., Rannala, B., 2010. Bayesian species delimitation using multilocus sequence data. P.

813   Natl. Acad. Sci-Biol. 107, 9264–9269.

814   Yang, Z., Rannala, B., 2014. Unguided species delimitation using DNA sequence data from

815   multiple loci. Mol. Biol. Evol. 31, 3125–3135.

816   Yu, Y., Barnett, R.M., Nakhleh, L., 2013. Parsimonious inference of hybridization in the

817   presence of incomplete lineage sorting. Syst. Biol. 62, 738–751.

818   Yu, Y., Dong, J., Liu, K.J., Nakhleh, L., 2014. Maximum likelihood inference of reticulate

819   evolutionary histories. Natl. Acad. Sci-Biol. 111, 16448–16453.

820   Zieliński, P., Nadachowska-Brzyska, K., Wielstra, B., Szkotak, R., Covaciu-Marcov, S.D.,

821   Cogălniceanu, D., Babik, W., 2013. No evidence for nuclear introgression despite

822   complete mtDNA replacement in the Carpathian newt (*Lissotriton montandoni*). Mol.

823   Ecol. 22, 1884–1903.

824   Zieliński, P., Stuglik, M.T., Dudek, K., Konczal, M., Babik, W., 2014. Development,

825   validation and high-throughput analysis of sequence markers in nonmodel species. Mol.

826   Ecol. Resour. 14, 352–360.

827   Zieliński, P., Nadachowska-Brzyska, K., Dudek, K., Babik, W., 2016. Divergence history of

828   the Carpathian and smooth newts modelled in space and time. Mol. Ecol. 25, 3912–3928.

829 **Table 1**. Joint Bayesian species delimitation and species tree estimation in the *Lissotriton*

830 *vulgaris* species group using BPP. Rows show results for different analyses; letters denote

831 replicate runs differing only by seed number. Population size (θ) and divergence time (τ)

832 priors encompass a wide range of demographic and divergence scenarios. Starting guide tree

833 topologies were random unless specified otherwise (see footnotes). *N* species shows the

834 numbers of species and their posterior probabilities (PPs) in each analysis (PPs for each

835 species within analyses were always 1.00). *N* trees denotes the number of trees in the 95%

836 credibility set, and the last column shows the topology and posterior probability of the highest

837 ranked tree in the set.

838

839

Runs	Θ[a]	τ[a]	*N* species (PP)	*N* trees	best tree and pp of model (delimitation + tree)
1a	G(1, 35)	G(2, 500)	9 (1.00)	7	(*L. graecus*, (*L. lantzi*, ((*L. schmidtleri*, *L. kosswigi*), ((S *L. v. vulgaris*, *L. v. meridionalis*), (N *L. v. vulgaris*, (*L. montandoni*, *L. v. ampelensis*)))))); 0.70905
1b	G(1, 35)	G(2, 500)	9 (1.00)	4	(*L. graecus*, (*L. lantzi*, (*L. kosswigi*, ((S *L. v. vulgaris*, *L. v. meridionalis*), (*L. schmidtleri*, (N *L. v. vulgaris*, (*L. montandoni*, *L. v. ampelensis*))))))); 0.83335
2a[b]	G(1, 35)	G(2, 500)	9 (1.00)	4	(*L. graecus*, (*L. lantzi*, (*L. kosswigi*, ((S *L. v. vulgaris*, *L. v. meridionalis*), (*L. schmidtleri*, (N *L. v. vulgaris*, (*L. montandoni*, *L. v. ampelensis*))))))); 0.81770
2b[b]	G(1, 35)	G(2, 500)	9 (1.00)	2	(*L. graecus*, (*L. lantzi*, (*L. kosswigi*, ((S *L. v. vulgaris*, *L. v. meridionalis*), (*L. schmidtleri*, (N *L. v. vulgaris*, (*L. montandoni*, *L. v. ampelensis*))))))); 0.88070
3a[c]	G(1, 35)	G(2, 500)	9 (1.00)	3	(*L. graecus*, (*L. lantzi*, (*L. kosswigi*, ((S *L. v. vulgaris*, *L. v. meridionalis*), (*L. schmidtleri*, (N *L. v. vulgaris*, (*L. montandoni*, *L. v. ampelensis*))))))); 0.82170
3b[c]	G(1, 35)	G(2, 500)	9 (1.00)	2	(*L. graecus*, (*L. lantzi*, (*L. kosswigi*, ((S *L. v. vulgaris*, *L. v. meridionalis*), (*L. schmidtleri*, (N *L. v. vulgaris*, (*L. montandoni*, *L. v. ampelensis*))))))); 0.85825
4a[d]	G(1, 35)	G(2, 500)	9 (1.00)	3	(*L. graecus*, (*L. lantzi*, (*L. kosswigi*, ((S *L. v. vulgaris*, *L. v. meridionalis*), (*L. schmidtleri*, (N *L. v. vulgaris*, (*L. montandoni*, *L. v. ampelensis*))))))); 0.79815
4b[d]	G(1, 35)	G(2, 500)	9 (1.00)	38	(*L. graecus*, (*L. lantzi*, (*L. kosswigi*, ((S *L. v. vulgaris*, *L. v. meridionalis*), (*L. schmidtleri*, (N *L. v. vulgaris*, (*L. montandoni*, *L. v. ampelensis*))))))); 0.43710
5a	G(1, 10)	G(2, 2000)	9 (1.00)	9	(*L. graecus*, (*L. lantzi*, (*L. kosswigi*, (*L. v. meridionalis*, (*L. schmidtleri*, ((*L. montandoni*, *L. v. ampelensis*), (N *L. v. vulgaris*, S *L. v. vulgaris*))))))); 0.33805
5b	G(1, 10)	G(2, 2000)	9 (1.00)	5	(*L. graecus*, (*L. lantzi*, (*L. kosswigi*, ((S *L. v. vulgaris*, *L. v. meridionalis*), (*L. schmidtleri*, (N *L. v. vulgaris*, (*L. montandoni*, *L. v. ampelensis*))))))); 0.71930
6a	G(2,2000)	G(2,2000)	9 (1.00)	50	(*L. v. meridionalis*, (((*L. graecus*, *L. lantzi*), (S *L. v. vulgaris*, (*L. montandoni*, *L. v. ampelensis*))), (N *L. v. vulgaris*, (*L. schmidtleri*, *L. kosswigi*)))); 0.13655
6b	G(2,2000)	G(2,2000)	9 (1.00)	45	((*L. graecus*, *L. lantzi*), ((*L. schmidtleri*, *L. kosswigi*), ((S *L. v. vulgaris*, *L. v. meridionalis*), (N *L. v. vulgaris*, (*L. montandoni*, *L. v. ampelensis*))))); 0.12370
7a	G(1, 10)	G(1, 10)	9 (1.00)	3	(*L. graecus*, (*L. lantzi*, (*L. kosswigi*, ((S *L. v. vulgaris*, *L. v. meridionalis*), (*L. schmidtleri*, (N *L. v. vulgaris*, (*L. montandoni*, *L. v. ampelensis*))))))); 0.66405
7b	G(1, 10)	G(1, 10)	9 (1.00)	5	(*L. graecus*, (*L. lantzi*, ((*L. schmidtleri*, *L. kosswigi*), ((S *L. v. vulgaris*, *L. v. meridionalis*), (N *L. v. vulgaris*, (*L. montandoni*, *L. v. ampelensis*)))))); 0.77125
8a	G(1, 10)	G(2,1000)	9 (1.00)	3	(*L. graecus*, (*L. lantzi*, ((*L. schmidtleri*, *L. kosswigi*), ((S *L. v. vulgaris*, *L. v. meridionalis*), (N *L. v. vulgaris*, (*L. montandoni*, *L. v. ampelensis*)))))); 0.80270
8b	G(1, 10)	G(2,1000)	9 (1.00)	9	(*L. graecus*, (*L. lantzi*, (*L. kosswigi*, ((S *L. v. vulgaris*, *L. v. meridionalis*), (*L. schmidtleri*, (N *L. v. vulgaris*, (*L. montandoni*, *L. v. ampelensis*))))))); 0.48025

840 [a] - G(1, 35), G(2, 500): empirically derived priors; G(1, 10), G(2, 2000): large populations

841 with shallow divergence; G(2,2000), G(2,2000): small populations with shallow divergence;

842 G(1, 10), G(1, 10): large populations with deep divergence; G(1, 10), G(2,1000): large

843 populations with intermediate divergence

844 [b] - starting tree according to consensus phylogeny

845 [c] - starting tree reflects gene flow among *L. montandoni*, *L. v. ampelensis* and N *L. v. vulgaris*

846 [d] - starting tree reflects gene flow among N *L. v. vulgaris* and S *L. v. vulgaris*, basal position

847   of *L. lantzi*

848 **Table 2.** Ensemble genealogical sorting index (*egsi*) for *Lissotriton* operational taxonomic

849 units (10 alleles per group) based on 70 gene trees. All of the P values for *egsi* are <0.000001.

850 The last column provides the number of gene trees in which a group reached complete

851 monophyly.

group	egsi	monophyly
L. lantzi	0.692	27
L. kosswigi	0.679	30
L. graecus	0.564	17
L. schmidtleri	0.559	14
L. montandoni	0.548	16
L. v. meridionalis	0.497	7
L. v. ampelensis	0.349	0
South *L. v. vulgaris*	0.343	0
North *L. v. vulgaris*	0.281	0

852

853 **Table 3.** Evaluation of fit of mtDNA sequence data to scenarios of incomplete lineage sorting

854 (ILS) and hybridization (Hyb). *Lva – L. v. ampelensis*; *Lg – L. graecus*; *Lk – L. kosswigi; Lvm*

855 *– L. v. meridionalis; Lm – L. montandoni; Ls – L. schmidtleri*; N*Lvv* – North *L. v. vulgaris*;

856 S*Lvv* – South *L. v. vulgaris*

Scenario	Pair of lineages	Minimum divergence - Observed	Minimum divergence – Expected (median of 1000 simulations)	P	Interpretation
mtDNA introgression into *L. montandoni*					
ILS	*Lm-Lva*	0.0020	0.0010	0.258	O = E
	Lm -NLvv	0.0000	0.0020	0.294	O = E
	Lm -Lk	0.0384	0.0020	0.002	O > E
	Lva-NLvv	0.0020	0.0010	0.220	O = E
	Lva-Lk	0.0207	0.0020	0.006	O > E
	NLvv-Lk	0.0374	0.0030	0.002	O > E
	Combined (Fisher's method)			0.00002	data do not fit scenario
Hyb1 *Lm -Lva*	*Lm -Lva*	0.0020	0.0010	0.034	
	Lm -NLvv	0.0000	0.0010	0.500	O = E
	Lm -Lk	0.0384	0.0098	0.046	O > E
	Lva-NLvv	0.0020	0.0010	0.242	O = E
	Lva-Lk	0.0207	0.0098	0.150	O = E
	NLvv-Lk	0.0374	0.0108	0.066	O = E
	Combined (Fisher's method)			0.0095	data do not fit scenario
Hyb2 *Lm -NLvv*	*Lm -Lva*	0.0020	0.0020	0.514	O = E
	Lm -NLvv	0.0000	0.0000	0.318	O = E
	Lm -Lk	0.0384	0.0089	0.040	O > E
	Lva-NLvv	0.0020	0.0020	0.824	O = E
	Lva-Lk	0.0207	0.0089	0.110	O = E
	NLvv-Lk	0.0374	0.0098	0.056	O = E
	Combined (Fisher's method)			0.0561	data fit scenario
mtDNA introgression into *L. graecus*					
ILS	*Lg -SLvv*	0.0000	0.0049	0.006	O < E
	Lg -Lvm	0.0139	0.0059	0.120	O = E
	Lg -Ls	0.0208	0.0059	0.036	O > E
	SLvv-Lvm	0.0069	0.0039	0.164	O = E
	SLvv-Ls	0.0139	0.0049	0.042	O > E
	Lvm-Ls	0.0396	0.0069	0.022	O > E
	Combined (Fisher's method)			0.0001	data do not fit scenario
Hyb *Lg-SLvv*	*Lg-SLvv*	0.0000	0.0020	0.180	O = E
	Lg-Lvm	0.0139	0.0069	0.086	O = E
	Lg-Ls	0.0208	0.0118	0.212	O = E
	SLvv-Lvm	0.0069	0.0069	0.832	O = E
	SLvv-Ls	0.0139	0.0118	0.560	O = E
	Lvm-Ls	0.0396	0.0138	0.080	O = E
	Combined (Fisher's method)			0.1152	data fit scenario

857

858   **Figure 1.** Map with ranges of morphological subspecies (A). Delimitation of evolutionary

859   lineages in the *Lissotriton vulgaris* species group in STRUCTURE (B). Pie charts show mean

860   individual cluster membership coefficients. *Lg – L. graecus; Lk – L. kosswigi; Ll – L. lanzti;*

861   *Lm – L. montandoni; Ls – L. schmidtleri; Lva – L. v. ampelensis; Lvm – L. v. meridionalis;*

862   *NLvv – North L. v. vulgaris; SLvv – South L. v. vulgaris*

863   **Figure 2.** Phylogenetic relationships among STRUCTURE-delimited groups of *Lissotriton*

864   newts; most genetic groups correspond to morphologically defined subspecies (except for *L.*

865   *v. vulgaris* that is split into northeastern and southwestern lineages and *L. v. ampelensis* which

866   contains two morphologies; see text for details). (A) Majority-rule consensus tree based on 10

867   replicate analyses (Fig. S4) of 74 concatenated nuclear loci for a total of 36,918 bp; values

868   designate the frequencies of clades found across replicates. Filled circles at nodes indicate

869   congruence across concatenation, concordance and TreeMix analyses. (B) Majority-rule

870   consensus of 50 primary concordance trees. Frequency of clades over all replicates (top

871   number) and concordance factors shown as the mean number of loci (out of 70) supporting

872   the clade (± SD). (C) Maximum likelihood tree as inferred by Treemix based on 355 SNPs;

873   horizontal branch lengths are proportional to the amount of genetic drift that has occurred in

874   each lineage. (D) Inferred evolutionary relationships among newt groups by TreeMix with

875   one (left), two (middle) and three (right) migration events. The migration arrows are coloured

876   according to their weights; the weight is correlated with the ancestry fraction.

877   **Figure 3.** Top: pairwise d_{xy} distances among *Lissotriton* taxa. Bottom: proportion (in percent,

878   left y-axis and solid circles) of shared haplotypes out of total number of haplotypes summed

879   for each taxon pair across 74 markers; values above solid circles indicate the number of

880   alleles shared by each taxon pair. Note that taxon pairs are in the same order on both charts.

881   *Lg – L. graecus; Lk – L. kosswigi; Ll – L. lanzti; Lm – L. montandoni; Ls – L. schmidtleri;*

882   *Lva – L. v. ampelensis; Lvm – L. v. meridionalis; NLvv – North L. v. vulgaris; SLvv – South L.*

883   *v. vulgaris*

884   **Figure 4.** Pie charts representing posterior distributions of Approximate Bayesian

885   Computation analyses in pairwise taxon comparisons (A), color coded according to

886   demographic models (inset in A). *Lissotriton vulgaris* group phylogeny showing well-

887   supported instances of post-divergence gene flow (green arrows) and their corresponding

888   posterior distributions from the ABC analyses (B).

889   **Figure 5.** Parameters of species trees under competing scenarios of incomplete lineage

890   sorting (ILS) and hybridization (HYB). Both θ and τ are measured as the expected number of
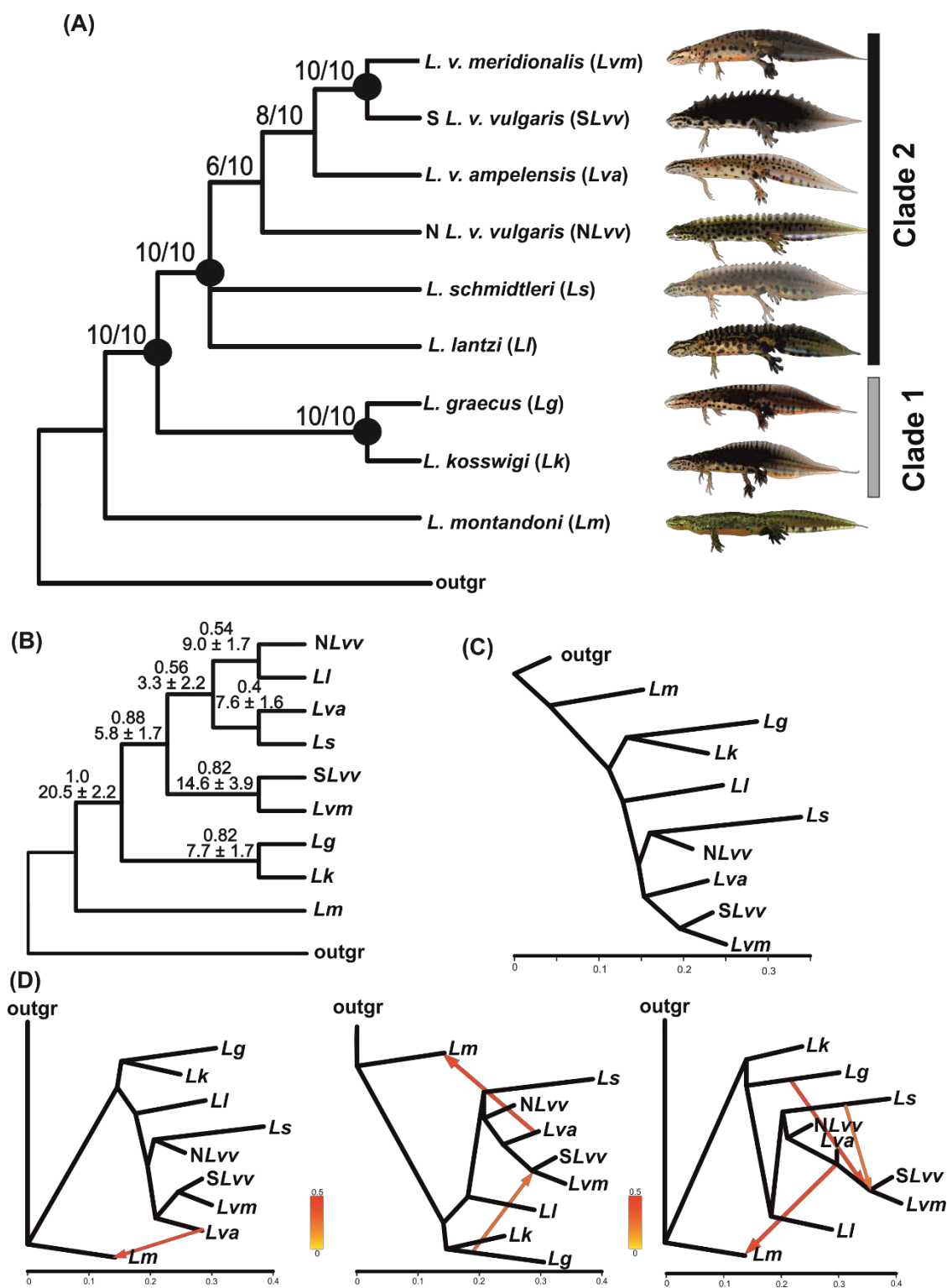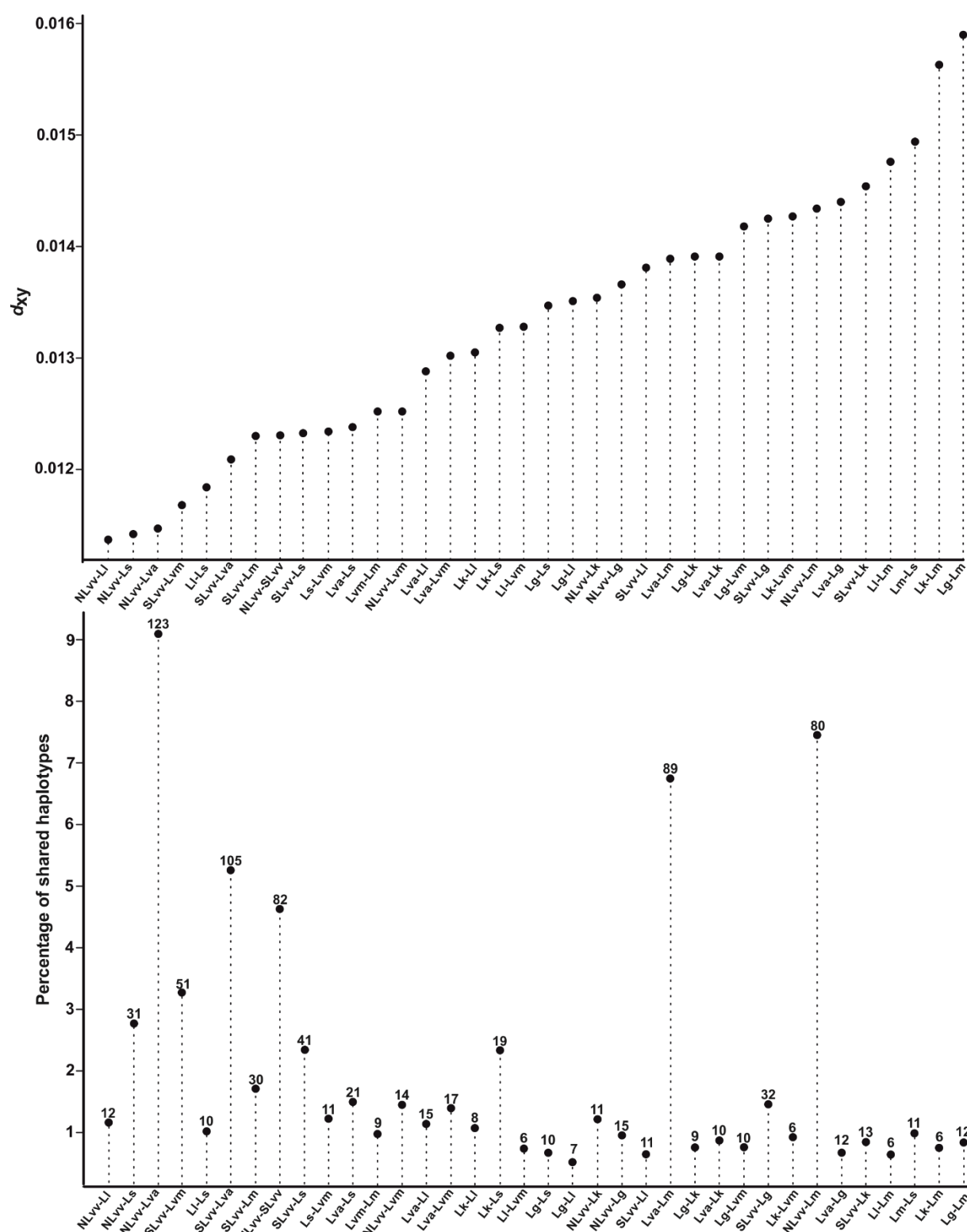
891   mutations per site.

43

892

893 **Fig. 1.**

894

895 **Fig. 2.**

45

896

897

Fig. 3.

899

Fig. 4

47

a) mtDNA introgression
into *L. montandoni*

b) mtDNA introgression
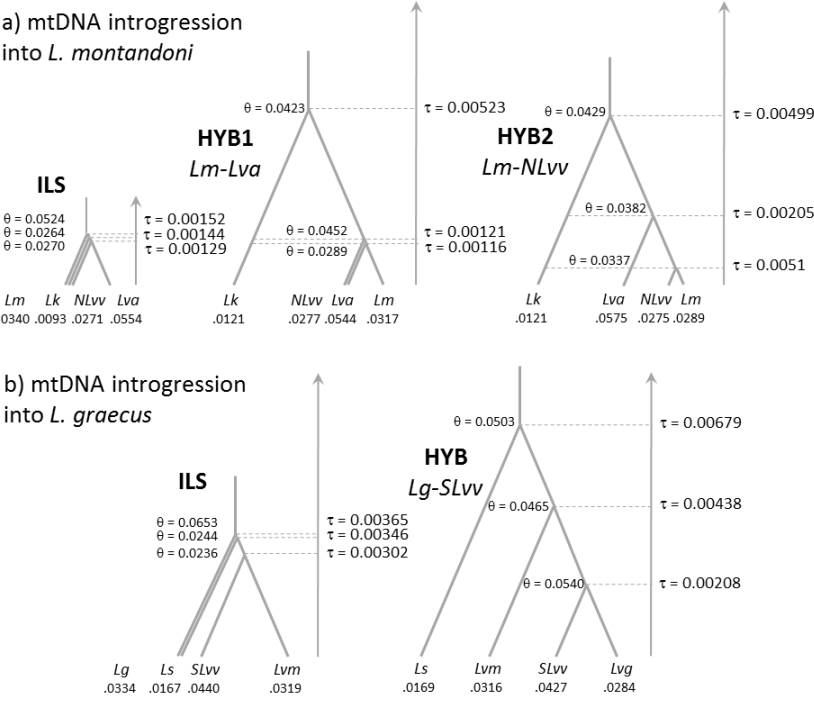into *L. graecus*

902
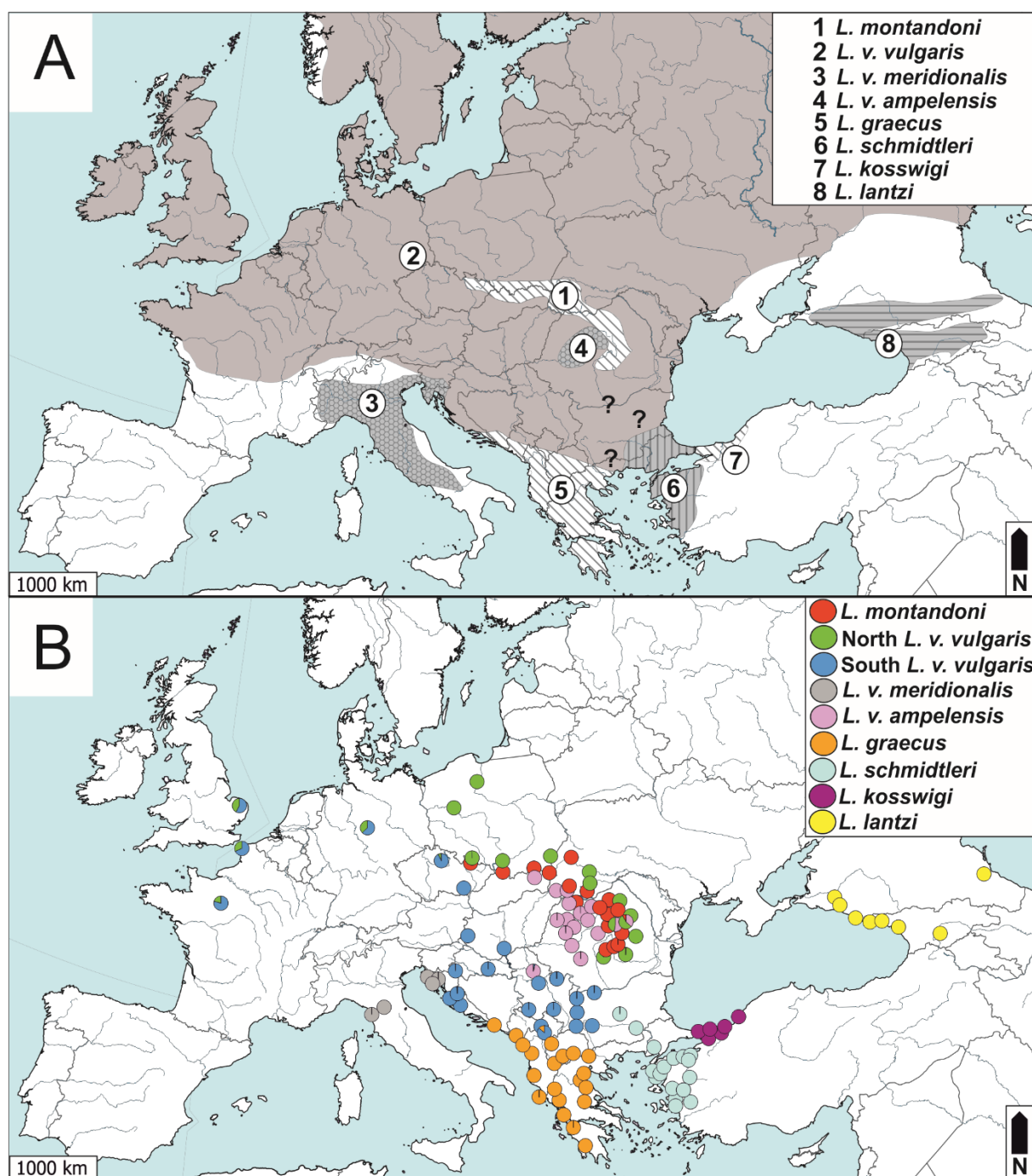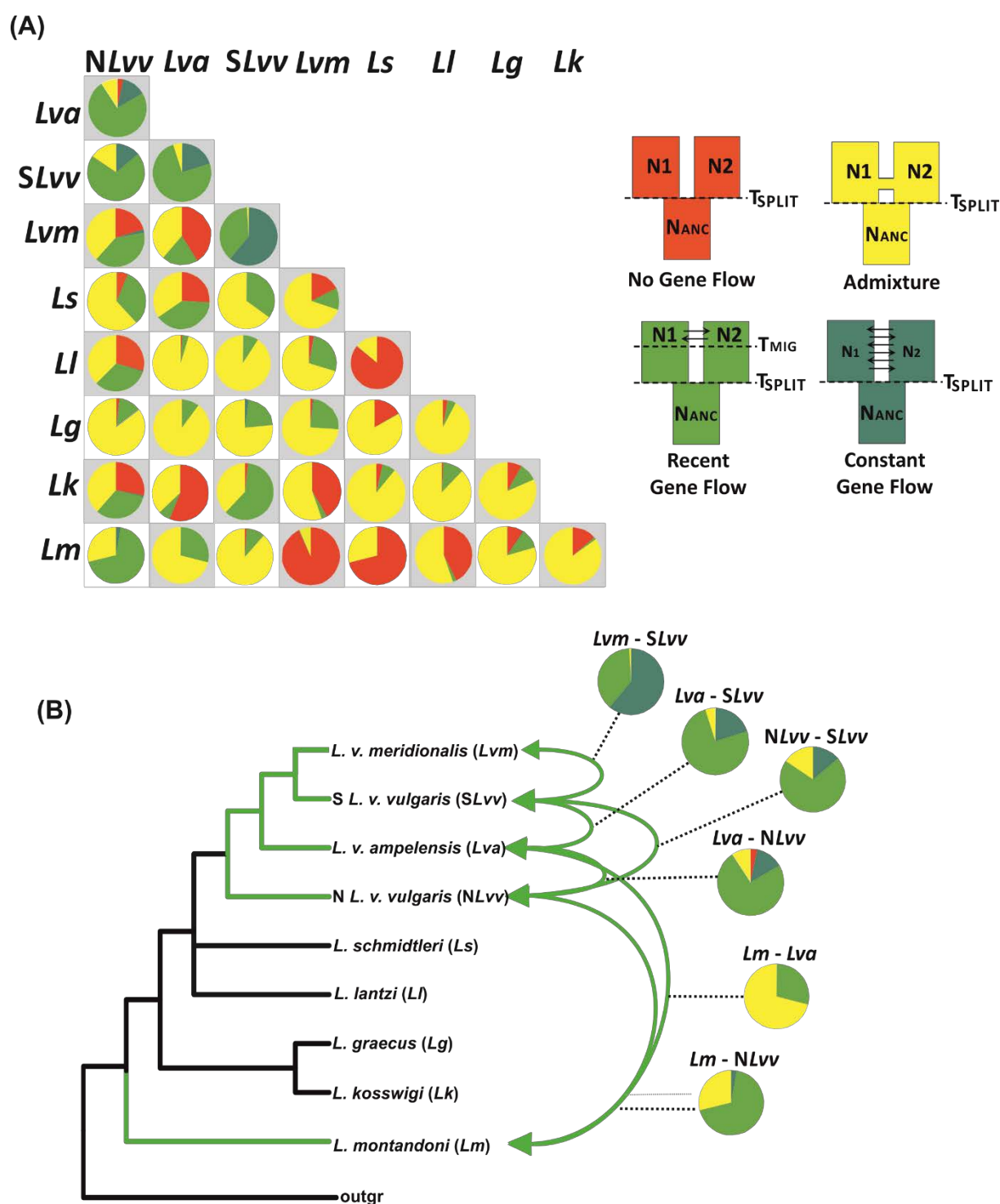
903 **Fig. 5**

SUPPORTING INFORMATION

Extended Methods: Validation of OTUs in BPP, phylogenetic analysis using BUCKy, and ABC analyses.

Table S1. A list of newt specimens with individual ID numbers, morphological species designation, geographical provenance and estimated proportion of genes in STRUCTURE-defined genetic clusters (c1-c9) representative of the species delimitation proposed in this study.

Table S2. Datasets used for species delimitation and phylogenetic reconstruction.

Table S3. Summary statistics for pairwise comparisons of *Lissotriton* taxa used in Approximate Bayesian Computation analyses.

Table S4. Summary of the nucleotide variation in 74 nuclear markers (mostly 3' UTR regions) in *Lissotriton vulgaris* (including all lineages delimited herein) and *L. montandoni*.

Table S5. Summary of STRUCTURE results for $K = 7\text{-}12$, iterated 10 times each for a total of 60 separate analyses.

Table S6. Pairwise matrix of d_{xy} values calculated for newt OTUs.

Table S7. Results of Approximate Bayesian Computation analyses under four demographic models: no gene flow (NGF), constant gene flow after divergence (CGF), recent (<200 kya) gene flow (RGF), and instantaneous admixture after divergence (ADM).

Table S8. Power analysis for Approximate Bayesian Analyses.

Table S9. Prior and posterior distributions for best model in pairwise taxon comparisons in *Lissotriton* newts from ABC analyses.

926   **Figure S1**. Relationships among major mtDNA lineages (denoted by capital letters) in

927   *Lissotriton,* modified from Pabijan et al. (2015).

928   **Figure S2**. Estimated *Ln* probability of the data for a given *K*, from STRUCTURE

929   HARVESTER; ten replicate analyses were run for each *K*.

930   **Figure S3**. Additional substructure found within South *L. v. vulgaris* and *L .graecus*.

931   **Figure S4.** Consensus trees from 10 replicates of concatenated analyses in MrBayes.

932   **Figure S5.** Variation in concordance factors (expressed as the number of genes supporting a

933   particular clade) for main clades found in 50 replicate BUCKy analyses.

934   **Figure S6.** Scaled residual fit from the TreeMix analysis based on the maximum likelihood

935   tree in Fig. 2C (no migration edges).